Published in final edited form as:
Exp Hematol. 2013 April ; 41(4): 398–408.e2. doi:10.1016/j.exphem.2012.11.007.

Development of membrane mechanical function during terminal stages of primitive erythropoiesis in mice

Richard E. Waugh[a], **Yu-Shan Huang**[b], **Binish J. Arif**[a], **Richard Bauserman**[a], and **James Palis**[b]

[a]Department of Biomedical Engineering, University of Rochester Medical Center, Rochester, NY

[b]Department of Pediatrics, Center for Pediatric Biomedical Research, University of Rochester Medical Center, Rochester, NY

Abstract

During murine embryogenesis, primitive erythroblasts enter the circulation as immature nucleated cells and progressively mature as a semisynchronous cohort, enucleating between E12.5 and E16.5. In this report, we examine the mechanical properties of these cells to determine how their mechanical development differs from that of definitive erythroid cells, which mature extravascularly in protected marrow microenvironments. Primitive erythroid cells acquire normal membrane deformability by E12.5 (i.e., as late stage erythroblasts) and maintain the same level of surface stiffness through E17.5. During this same period, the strength of association between the membrane bilayer and the underlying skeleton increases, as indicated by an approximate doubling of the energy required to separate bilayer from skeleton. At the same time, these cells undergo dramatic changes in surface area and volume, losing 35% of their surface area and 50% of their volume from E14.5 to E17.5. Interestingly, membrane remodeling proceeded regardless of whether the cells completed enucleation. These data suggest that in primitive erythroid cells, unlike their definitive counterparts, the critical maturational processes of membrane remodeling and enucleation are uncoupled.

Examination of mammalian embryos a century ago revealed the circulation of distinct but overlapping populations of nucleated and enucleated erythroid cells [1]. The former consisted of a transient population of large cells that originated in the yolk sac and were termed *primitive* because of the association of nucleated red blood cells (RBCs) with birds, reptiles, and fish [2]. This population was subsequently superseded by a population of smaller cells, termed *definitive* because they resembled the enucleated RBCs found throughout postnatal life in mammals. We previously determined that primitive erythroid cells emerge in the mouse embryo from a transient population of lineage-committed progenitors [3] and subsequently mature as a semisynchronous cohort in the bloodstream [3,4]. More recently, we recognized that primitive erythroblasts ultimately enucleate [5,6] like their definitive counterparts; this process is unique to mammalian erythropoiesis. Thus, there are many parallels between the maturational programs for primitive and definitive erythroid lineages, but there are also clear differences. In contrast to definitive erythropoiesis, in which reticulocytes enter the circulation after enucleating, primitive

Offprint requests to: James Palis, M.D., Department of Pediatrics, Center for Pediatric Biomedical Research, Box 703, University of Rochester Medical Center, 601 Elmwood Avenue, Rochester, NY 14642; James_Palis@urmc.rochester.edu.

Supplementary data related to this article can be found online at http://dx.doi.org/10.1016/j.exphem.2012.11.007.

Conflict of interest disclosure: No financial interest/relationships with financial interest relating to the topic of this article have been declared.

erythroid cells enter the newly formed bloodstream as immature erythroid precursors and continue to circulate as they progressively mature [6]. Understanding how this difference affects the development of primitive erythroid cells provides insights into mechanisms underlying the development of functional RBCs in normal and pathologic situations.

One of the principal requirements for RBC viability is sufficient deformability and mechanical stability to negotiate the vasculature. Indeed, it is well documented that abnormalities in structural proteins leading to altered mechanical behavior are the underlying cause of many forms of hemolytic anemia [7,8]. Therefore, understanding the development of proper mechanical function during erythroid maturation is of fundamental importance for understanding hemolytic pathology. Prior studies of mechanical function in definitive erythroid cells have focused primarily on changes in deformability during late-stage maturation. Early studies suggested that increased deformability during reticulocyte maturation might contribute to their regulated release from the marrow into the circulation. LeBlond et al [9] demonstrated increased rigidity of definitive normoblasts and reticulocytes in mice and humans [9]. Others have shown a marked reduction in cell surface area during reticulocyte maturation [10,11] as unneeded receptors are selectively endocytosed and expelled from the cell [12]. Although immature definitive erythroid cells tend to be less deformable than their mature counterparts are, their membranes are less stable mechanically [13,14]. This membrane instability can be tolerated by definitive erythroid cells because they mature in a mechanically protected extravascular environment, including the fetal liver and postnatal bone marrow or spleen. It is of interest to understand how the mechanical properties of primitive erythroid cells change during maturation, and what accommodations, if any, this embryonic erythroid lineage has implemented because of its need to undergo maturation while functioning within the fetal circulation.

We focus on three properties of the primitive erythroid cells and how they change during terminal maturation. First, the ratio of the membrane area to the cell volume is a critical determinant of the cell's ability to survive in the vasculature. Second, the elastic “shear” stiffness of the membrane arises from the membrane-associated cytoskeleton and provides an indication of its proper assembly. Third, the strength of association between the membrane bilayer and the underlying cytoskeleton determines the ability of the cell to maintain the integrity of the membrane bilayer and its surface area. We find that primitive erythroblasts and erythrocytes exhibit levels of membrane stability and deformability that are consistent with the fact that they are circulating cells. Furthermore, whereas primitive erythroid cells undergo dramatic and synchronized reductions in size that are consistent with a mammalian erythroid maturational program, these changes are independent of their enucleation status.

Methods

Cell collection

ICR mice (Taconic, Germantown, NY, USA) were mated overnight, and vaginal plugs examined in the morning, considered embryonic day (E) 0.3. At specified times during gestation E12.5–E17.5, mice were killed by CO_2 inhalation and embryonic tissues were dissected in PB2 (Dulbecco PBS [Gibco-Brl, Gaithersburg, MD], 0.3% BSA [Gemini Bio-Products, Sacramento, CA, USA], 0.68 mmol/L $CaCl_2$ [Sigma-Aldrich, St Louis, MO, USA], 0.1% glucose). Fetal blood was collected as described previously [6].

Biotinylation of cells

For membrane stability measurements by tether formation, primitive erythroid cells were biotinylated with NHS biotin (Pierce Chemical, Rockford, IL, USA). Biotin was dissolved at

10 mg/mL in dimethyl sulfoxide then diluted into whole blood 1:1000 to make a concentration of 10 μg/mL. After mixing in the dark for 5 min, cells were centrifuged and washed twice in PBS (160 mmol/L NaCl, 6.2 mmol/L KH_2PO_4, 25 mmol/L Na_2HPO_4, 290 mOsm) and twice in hypotonic (155 mOsm) PBS.

CD9 labeling

Fetal blood cells (10^6 cells) were resuspended in 50 μL of 2% BSA in PB2 and incubated on ice for 15 min. PB2 (50 μL) containing 1 μL of anti-CD9 antibody (eBioscience, San Diego, CA; catalog no. 12-0091-81) was added to the cells. After a 20-min incubation at 37°C, the cells were washed in PB2 and analyzed by microscopy.

Imaging flow cytometry

Fetal blood cells (5×10^6 cells) from E12.5, E14.5, and E16.5 mouse embryos were each resuspended in 50 μL of 10% rat whole serum (Invitrogen, Carlsbad, CA) and stained with 1 μL of Ter119-PE-Cy7 and CD71-FITC (eBioscience) on ice for 20 min in the dark. Cells were washed and stained with 0.625-1.25 μmol/L of DRAQ5 (Biostatus, Shepshed, Leicestershire, UK) and imaged using the ImageStreamX (Amnis, Seattle, WA). Data were analyzed using ImageStream Data Exploration and Analysis Software (IDEAS; Amnis). Debris and cell aggregates were excluded, and individual cells were identified by gating on size and aspect ratio. Co-circulating primitive and definitive erythroid cells were identified using size and Ter119 staining intensity (Supplementary Figure S1, online only, available at www.exphem.org).

Area and volume measurements

Cells were aspirated into a glass micropipette at a pressure of approximately 1,500 Pa (15 cm H_2O) to ensure that the membrane was fully extended into the pipette (Fig. 1A). Care was taken that there were no folds or creases in the membrane projection. The cell area A and the cell volume V were calculated from measurements of the outer cell radius, R_c and the length of the projection in the pipette, L_p:

$$A = 2\pi R_c \left(R_c + \sqrt{R_c^2 - R_p^2} \right) + 2\pi R_p L_p \quad (1)$$

$$V = \frac{2\pi}{3} \left[R_o^3 + \left(R_o^2 + \frac{R_p^2}{2} \right) \sqrt{R_o^2 - R_p^2} + R_p^3 \right] + \pi R_p^2 (L_p - R_p) \quad (2)$$

The sphericity of the cell S is a dimensionless quantity proportional to the ratio of the 2/3 power of the volume to the cell area [15]:

$$S = \frac{4\pi}{(4/3\pi)^{2/3}} \cdot \frac{V^{2/3}}{A} \quad (3)$$

The coefficient makes the maximum value of the sphericity 1.0 a perfect sphere. The smaller the sphericity value, the greater the “excess” surface area of the cell—that is, the area in excess of the area required to enclose the spherical volume of the cell.

Shear modulus measurements

A single cell was aspirated on a “flat” region of the surface (Fig. 1B) and positioned in the field of view. A series of aspiration pressures was applied in the range of 15–60 Pa (1.5–6.0

mm H_2O pressure, approximately) and the length of the cell projection in the pipette was measured as a function of the applied pressure. An effective elastic shear modulus was calculated according to the theory originally set forth by Evans and Shalak [16]. The modulus is approximately related to the slope of the length, pressure data pairs by [17]:

$$\mu = \frac{R_p^2}{2.45} \cdot \frac{dP}{dL_p} \quad (4)$$

where L_p is the length of the membrane projection into the pipette, P is the pressure difference between the pipette and the suspending fluid, R_p is the pipette radius, and μ is the modulus.

Tether formation measurements

Biotinylated cells and streptavidin-coated beads were combined and placed in a chamber on the stage of an inverted microscope. The chamber allowed access from two directions, one for the cell manipulating pipette, and one for a much longer and thinner pipette that served as a microcantilever (Fig. 1C). The aspiration pressure in the pipettes was controlled via a water manometer. The manipulating pipette was used to capture a cell and bring it into contact with the bead held in the tip of the cantilever, forming an adhesive contact. The cell was withdrawn, forming a tether between the bead and the cell body (Fig. 1C). As the tether formed, the cantilever was deflected, the magnitude of the deflection being proportional to the force on the tether. Once a tether was formed, the pressure in the pipette was incremented in steps, allowing 1–3 min for the tether to come to equilibrium before changing to the next pressure. Video images included the time, date and aspiration pressure and were stored for subsequent analysis. The cell dimensions, the cantilever deflection, and the aspiration pressure were obtained from the images. The force on the tether was calculated from the deflection of the microcantilever, and the relationship between tethering force and aspiration pressure was used to calculate the energy needed to separate the bilayer from the membrane skeleton.

Calibration of glass microcantilevers

Microcantilevers were formed from capillary tubing pulled under high heat to produce a long (~5 mm), hairlike, but hollow, flexible tip. The relationship between the force on the fiber and its deflection was determined by attaching a cell-bead pair to the tip of the fiber, then using a large pipette to suck the cell completely inside at a series of increasing pressures. The pipette was withdrawn until the tip no longer contacted the fiber, such that there was an equilibrium between the aspiration pressure pulling the cell into the pipette and the force of the deflected fiber on the attached bead. The force is given by:

$$f = \pi R_p^2 \Delta P \quad (5)$$

where R_p is the pipette radius and ΔP is the aspiration pressure.

Calculations

Consideration of the equilibrium between a bilayer tether and the contiguous bilayer on the surface of the cell reveals that the force needed to maintain a constant tether length has two contributions: one because of the mechanical tension in the membrane bilayer and one because of the natural energy of association between the membrane bilayer and the underlying cytoskeleton. Analysis of this equilibrium yields the following relationship between the tether force f and the bilayer tension τ_o [18]:

$$f^2 = 8\pi^2 k_c(\tau_o + W_{sk}) \quad (6)$$

where k_c is the bending stiffness of the membrane and W_{sk} is the energy required to separate the bilayer from the membrane skeleton. The basic strategy is to measure the force at a series of different bilayer tensions and extrapolate to zero tension to determine W_{sk}. In other words, we use the linear relationship given in Equation 5 to determine the zero-tension intercept, which is proportional to the energy of separation W_{sk}. The membrane tension on the cell body τ_m can be calculated from simple balance of forces:

$$\tau_m = \frac{\Delta P}{2}\left(\frac{1}{R_p} - \frac{1}{R_c}\right)^{-1} \quad (7)$$

where R_c represents the maximum radial dimension of the portion of the cell outside the pipette. This tension includes forces within the membrane bilayer and forces within the membrane skeleton. The bilayer tension τ_o can be approximated as the total membrane tension calculated by using Equation 6 in cases where the total tension is large compared with the stiffness of the membrane skeleton. However, when the forces applied to the cell are small, a more exact calculation is required that accounts for the contributions to the tension from the membrane skeleton. A good approximation of this takes the form:

$$\tau_o \approx \frac{R_p R_c}{2\left(R_c - R_p\right)}\left(\Delta P - \frac{f_t}{\pi R_c^2}\right) - \tau_{mp}^{sk} \quad (8)$$

where the quantity $\tau_{mp}{}^{sk}$ represents the axial tension in the skeleton at the tip of the pipette. The value of $\tau_{mp}{}^{sk}$ is estimated from the projection length of the cell and the membrane shear modulus according to:

$$\tau_{mp}^{sk} = 2.45\mu\left(\frac{L}{R_p} - \frac{L_o}{R_p}\right) \quad (9)$$

where μ is the shear modulus, and L_o/R_p is the intercept for $P = 0$ obtained from linear regression of measurements of L as a function of P during shear modulus measurements (described above). In Equation 8, L is the length of the cell projection in the pipette measured during tether formation. Using these relationships, the square of the force is determined as a function of the bilayer tension. In theory, the bending stiffness of the membrane can be determined from the slope of the resulting linear relationship, and the work of separation is determined from the intercept. In practice, the slope of the relationship may also be affected by unaccounted-for stiffness in the cell interior.

Results

Terminal maturation of primitive erythroid cells

We have previously determined that primitive erythroid cells mature as a semisynchronous cohort in the mouse embryo and enucleate between E12.5 and E16.5 of gestation [6]. To better characterize primitive erythroid cells during this transition from orthochromatic erythroblast (E12.5) to reticulocyte (E14.5–16.5), cellular features were analyzed with imaging flow cytometry. Primitive and definitive erythroid cells can be distinguished by combining quantitative analyses of cell size and Ter119 staining (Fig. 2A; Supplementary Figure S1, online only, available at www.exphem.org). At E12.5, almost all primitive

erythroid cells are nucleated, whereas at E14.5 and E16.5 both nucleated and enucleated primitive erythroid cell populations are evident (Fig. 2A). At E14.5, the enucleated primitive erythroid cell population was significantly smaller than their nucleated counterparts (Fig. 2B). By E16.5, the enucleated primitive erythroid cell population had decreased significantly in size, suggesting that membrane remodeling had taken place during reticulocyte maturation (Fig. 2B).

Reticulocyte maturation in definitive erythroid cells is characterized by the marked loss of CD71. We therefore analyzed the surface expression of CD71 on primitive erythroid cells at E12.5, 14.5, and 16.5 of gestation. As shown in Figure 2C, the newly formed primitive reticulocytes revealed a marked decrease in CD71 compared with the primitive orthochromatic erythroblasts examined at E12.5. Surprisingly, the nucleated primitive erythroid cells at E14.5 revealed similar kinetics and degrees of CD71 loss (Fig. 2C, black line). In addition, we noted that the small numbers of nucleated primitive erythro-blasts at E16.5 had a similar area with their enucleated counterparts (Fig. 2B). These data raise the possibility that membrane remodeling during the terminal maturation of primitive erythroid cells proceeds independently of nucleation status.

We also examined the developmental changes in Ter119 cell surface expression as primitive erythroid cells terminally mature. Primitive erythroid cells express significantly less Ter119 on their cell surface compared with their fetal definitive counterparts (Fig. 2A, 2D), but the subsequent rate of loss resembles what has been documented for glycophorin A in definitive erythroid cells [20]. Indeed, the loss of Ter119 staining between E14.5 and E16.5 roughly follows the proportion of membrane loss in both nucleated and enucleated cells over that time period (see Table 1), similar to what is observed in definitive reticulocytes [20]. However, Ter119 loss in primitive erythroid cells occurs regardless of whether the cell has enucleated, further supporting the notion that membrane remodeling and enucleation are proceeding as independent processes in these cells.

Changes in surface area and volume of late-stage primitive erythroid cells

To obtain a more precise measure of changes in cell size, cell samples ranging from E12.5 to E17.5 were tested using micropipettes. Primitive erythroid cells were labeled with a fluorescent marker for CD9, a molecule that is present on the surface of primitive erythroid cells but not on late-stage fetal definitive or maternal RBCs [21]. Staining with CD9 antibodies allowed us to identify objectively individual primitive erythroid cells from samples of fetal blood containing a mixture of primitive and definitive erythroid cells (Fig. 2E).

Surface area, volume, and sphericity were calculated as described in the Methods section. Before E15.5, all but a few cells were nucleated, but by E16.5, only a few cells contained nuclei (Fig. 3 and Table 1). The mean area and volume showed little change through E14.5, after which cell size decreased more or less linearly, resulting in the loss of 35% of the surface area and approximately 50% of the cell volume over 3 days (Fig. 3A, 3B). Part of this loss is attributable to enucleation. Comparing nucleated and enucleated cells at E15.5, enucleation results in a loss of approximately 6% of the cell area and 16% of the cell volume. The remainder of the change appears to be a consequence of membrane remodeling. Comparing enucleated primitive erythroid cells at E15.5 to enucleated cells at E17.5, cell area is reduced approximately 20%, with a corresponding 33% loss of cell volume. Remarkably, despite these enormous changes in area and volume, the ratio of the two, as reflected in the dimensionless cell sphericity, changes by less than 6% from E14.5 to E17.5 (Fig. 3C). This latter finding is consistent with prior studies that have indicated that sphericity is a tightly regulated characteristic of circulating erythroid cells [22]. Enucleated primitive erythroid cells at E14.5 and E15.5 are 2.0- to 2.25-fold larger than their definitive

counterparts, and at E16.5 and 17.5 are 70% to 80% larger than cells from the definitive erythroid lineage (see Supplementary Table S1, online only, available at www.exphem.org).

Shear modulus measurements

Primitive erythroid cells from E12.5 through E16.5 were tested for membrane rigidity using micropipettes. Measurements were performed on cells having a biconcave or mildly stomatocytic shape, which accounted for the vast majority of the cell population. In one set of measurements, primitive cells were unlabeled and were selected based on their size and appearance, and in another (for the same cell sample) they were selected on the basis of CD9 labeling. Representative examples of the relationship between projection length L (normalized to the pipette radius R_p) as a function of increasing pressure (scaled by R_p) are shown in Figure 4A. The stiffness of the membrane is reflected in the slopes of these data. Softer membranes have steeper slopes (greater increase in projection for a given increase in aspiration pressure), and stiffer membranes have lower slopes. The similarity of the slopes for the different types of cells shown in Figure 4A indicates that these cells all have similar stiffness. Indeed, two-way analysis of variance (ANOVA) analysis revealed no significant differences in shear modulus across all days or between the labeled and unlabeled cells (Fig. 4B). Nucleated cells were tested on all dates, and enucleated cells were tested at E15.5 and E16.5. On E15.5 and E16.5, there were no significant differences in shear modulus between nucleated and enucleated cells. The mean modulus for primitive erythroid cells across all days was 4.3 μN/m, with SD typically around 0.9 μN/m. It is remarkable that, despite the substantial reduction in cell area (indicative of significant membrane remodeling), the deformability of the cell membrane remains essentially constant throughout this period of development. The elastic modulus for the primitive erythroid cells was slightly smaller than the modulus for adult human RBCs (5.5 μN/m) measured under similar conditions, but was not statistically different from cells from the definitive erythroid lineage obtained from the same embryos.

Membrane stability

The third membrane characteristic we investigated was the stability of the association between the membrane bilayer and the membrane skeleton as assessed by tether formation. Cells from E12.5, E14.5, and E16.5 were tested. As shown in Figure 5A, the expected linear relationship between the square of the tether force and the membrane tension was observed. The most obvious change that occurs in primary primitive erythroid cells between E12.5 and E16.5 is an increase in the slope of the data. This change is most likely due to decreases in the mechanical stiffness of interior structure of the cell as it matures. Evidence for this conclusion comes from observations that during the tether experiment, the length of the projection in the pipette barely increased for E16.5 cells, a behavior consistent with the cell having low cytoskeletal stiffness, such that an increase in projection length is limited by the cell's fixed surface area and volume. In contrast, the projection length increased with pressure for E12.5 and E14.5 cells. The increase was greater for E12.5 than for E14.5, indicating a larger cytoskeletal contribution to the stiffness of these cells and which decreases with maturation after E12.5. These changes cannot be accounted for by membrane stiffness alone, which was found to be the same for all the different days of development; therefore, it would not account for the progressive differences in projection length change observed for different maturational states.

The conclusion that there is decreasing cytoskeletal contribution to cellular stiffness with increasing maturity is also supported by recent observations in adult reticulocytes that there is a progressive loss of actin and tubulin from the interior of reticulocytes [20]. Also consistent with these data, we have noted a progressive loss of mitochondria between E12.5 and E15.5 (J. Palis, unpublished observations). In addition to these observations, the small

changes in projection length observed for primitive erythroid cells at E16.5 indicate minimal internal structures in these cells. In the absence of internal structure, the slope of the lines in Figure 5 can be used to determine the membrane bending stiffness. The bending stiffness calculated for those data was 0.30 pN-μm, a value in reasonable agreement with those reported for human red blood cells [18,23].

The data also provide information about changes in the stability of the membrane-cytoskeletal association with maturation. Assuming that the membrane bending stiffness does not change with maturation, we can use the value of the bending stiffness obtained for E16.5 cells to calculate the change in the bilayer-skeletal separation energy for the different days. These results indicate a progressive increase in membrane stability with maturation, as the value estimated for the energy of separation nearly doubled from E12.5 to E16.5 from 30.4 pJ/μm^2 to 53.0 pJ/mm^2 (Fig. 5B and Table 2). These findings are consistent with reports of reduced membrane stability in late human erythroblasts and immature reticulocytes [13,14]. The membrane stability measured in definitive erythroid cells from an E14.5 embryo was slightly higher (W_{sk} = 65.6 ± 29.8 pJ/μm^2) than what was observed for primitive erythroid cells at E16.5 or E14.5, but the difference was not statistically significant; however, the mean separation energy for definitive erythroid cells at E14.5 and for primitive erythroid cells at E16.5 was significantly higher than what was observed for E12.5.

Discussion

Proper RBC deformability is essential for healthy circulation and oxygen delivery. In the mature RBC, the interior is a simple fluid and the structural stability resides entirely in the membrane. The membrane itself is a composite consisting of a phospholipid bilayer with embedded transmembrane proteins and a tightly membrane-associated cytoskeleton that resides at the cytoplasmic face of the bilayer. The bilayer behaves mechanically as a two-dimensional fluid—that is, it flows easily in the plane of the surface, but exhibits a high degree of stiffness, an almost crystalline character, in its resistance to change in surface area. This constraint on membrane area, coupled with constraints on the cell volume, combine to place strict limits on the ability of the cell to deform. Thus, a critical requirement for RBC survival is that the membrane area must be sufficiently large to enclose the cell volume as it negotiates the smallest capillaries and narrow passages in the microvasculature. The membrane-associated cytoskeleton in mature RBCs functions to stabilize the membrane bilayer against fragmentation so that an adequate membrane area is maintained. The elastic character of the membrane skeleton provides the cell with “shape memory,” enabling it to return to its natural biconcave shape after deformation, but this is soft resistance compared with the resistance of the membrane bilayer to area changes. Thus, the elastic resistance of the membrane skeleton must be sufficient to maintain cell cohesion under the shear stresses encountered in the vasculature, but low enough to enable the mature erythrocyte to deform easily within its constraints of fixed surface area and volume.

The importance of the proper assembly and stability of the membrane-associated cytoskeleton is evident in many cases of inherited hemolytic anemia, particularly those in which the genetic abnormality has been traced to proteins within the membrane-associated cytoskeleton, or to proteins important for maintaining cohesion between the cytoskeleton and the bilayer. It has been shown that the degree of severity of the anemia correlates with the degree of deficiency in spectrin [24], and this deficiency in turn correlates with reduction in the elastic shear modulus of the RBC membrane. It has also been shown that the strength of the bilayer skeletal association is also reduced in hereditary spherocytic anemia [23,25].

Primitive erythroid cells enter the circulation of mouse embryos between E8.5 and E9.5 as proerythroblasts and mature in the bloodstream as a semisynchronous cohort, reaching the orthochromatic stage of maturation by E12.5. This population of cells then enucleates over the subsequent 4–5 days of embryogenesis [5,6]. The finding that the membrane shear modulus does not change significantly in primitive erythroid cells between E12.5 and E16.5 was somewhat surprising. Indeed, nucleated and enucleated forms showed no difference in the forces required to produce membrane deformation. Despite the enormous structural changes taking place over this time-period, late-stage primitive erythroid cells manage to maintain consistent levels of surface deformability. This finding could indicate that primitive erythroblasts have already assembled a mature form of the membrane-associated cytoskeleton by E12.5 (i.e., prior to enucleation). An alternative explanation is that there is a well-controlled evolution of the membrane-associated cytoskeleton that enables the cell to transition from an early structure to a mature structure without significant changes in surface stiffness. Although the former seems more likely, a definitive selection between these alternatives must await further study.

Despite the fact that the surface shear modulus does not change during these late terminal stages of primitive erythroid cell maturation, we found evidence of a progressive increase in the stability of the association between the membrane bilayer and the underlying cytoskeleton. This finding is consistent with previous studies indicating that these two cell characteristics have different structural origins in RBCs [26]. Surface deformability depends on the presence of an elastic network of proteins at the cytoplasmic face of the bilayer. The membrane deformability depends on the flexibility of this network. Bilayer detachment, however, depends on the associations between integral membrane proteins in the bilayer and the subjacent cytoskeleton [23,26]. Thus, it appears that the network itself may be well formed in primitive erythroblasts by E12.5, but the associations between the bilayer and the cytoskeleton continue to evolve from E12.5 to E16.5. Values for the energy of separation are comparable to values that have been reported previously for mature human (60–90 $\mu J/m^2$) [18,23,27], and murine erythrocytes (~40 $\mu J/m^2$; Waugh et al., unpublished data). The conclusion that there is an evolution of bilayer-skeletal attachments during maturation of primitive erythroid cells is consistent with recent findings in adult mouse cells that the junctional complex organized around protein 4.1R is more labile in reticulocytes than in fully mature RBCs [20]. This conclusion appeared to be related to dephosphorylation of protein 4.1R and suggests a continued strengthening of the bilayer skeletal association as reticulocytes mature. It is also consistent with the lower membrane stability of human orthochromatic erythroblasts and early reticulocytes compared with mature RBCs [13,14]. The cytoskeletal composition of primitive erythroid cells has not been examined, and it will be of interest to determine whether there is a 4.1 isoform switch during the maturation of primitive erythroblasts and whether the phosphorylation state of protein 4.1 might also change during terminal erythroid cell maturation.

The most dramatic changes in cellular properties of primitive erythroid cells during late stages of maturation are the enormous reductions in surface area and volume that occur between E14.5 and E17.5; enucleation contributes to part of this. The extruded nucleus with its surrounding membrane, recently termed *pyrenocyte* [19], has a diameter of approximately 4.0 mm, giving it a surface area of approximately 50 mm^2 and a volume of approximately 33.5 μm^3. However, the difference in the mean area between nucleated and enucleated forms on E15.5 was only 23 μm^2, and the difference in the mean volume was 80 μm^3. Clearly these changes cannot be explained by the simple extrusion of the nucleus. The less than expected change in area may be due to the fusion of internal vesicles with the membrane during the enucleation process, as has been recently proposed for the enucleation of definitive erythroid cells [28]. The loss of surface area seen in late stage erythropoiesis can be attributed to the formation and release of exosomes as the membrane is remodeled to

remove a variety of integral proteins [20]. However, the volume loss we have observed in primary primitive erythroid cells cannot be ascribed solely to the formation and release of exosomes. For example, loss of surface area and volume between E14.4 and E15.5 is 48 μm^2 and 80 μm^3, respectively. If both of these losses resulted from exosome extrusion, and the exosomes had diameters of 60 nm, the loss of ~4,000 exosomes could account for the surface area loss, but this would account for a volume loss of only ~0.4 μm^3 [29]. Thus, other mechanisms, such as the loss of solutes and water through volume regulatory pathways, are likely responsible for the observed changes in cell volume.

Perhaps the most remarkable finding of the present study is the uncoupling of the enucleation process from membrane remodeling during primitive erythroid cell maturation. Lateral segregation of membrane components during enucleation contributes to the final composition of the reticulocyte membrane in adult cells, and abnormalities in this sorting lead to altered membrane composition associated with hereditary spherocytosis and hereditary elliptocytosis [30]. Our evidence suggests that this might not be a necessary step for primitive erythroid cell maturation. The presence of nucleated primitive erythroid cells in the embryonic circulation as late as E17.5, and the observation that these nucleated forms have surface areas and volumes indistinguishable from their enucleated counterparts, indicates that membrane remodeling in primitive erythroid cells proceeds effectively whether or not enucleation has occurred. The loss of CD71 between E12.5 and E14.5 (before the majority of enucleation), and the decline in Ter119 expression between E14.5 and E16.5 in both nucleated and enucleated cells also supports this interpretation. We hypothesize that the lateral segregation of membrane components leading to selective elimination of specific membrane proteins during enucleation may be disrupted in primitive erythroid cells as they circulate, reducing the fidelity of the process. However, the process of remodeling itself appears to depend on the cells remaining in the vasculature, because cells removed at E14.5 and kept in culture did not exhibit significant loss in membrane area over 48 hours (data not shown). Thus, the differences in the maturational process between definitive and primitive erythroid lineages might be explained by the fact that nucleated cells are in circulation, where membrane remodeling can proceed normally, but where protein segregation that normally occurs during enucleation is disrupted.

Supplementary Material

Refer to Web version on PubMed Central for supplementary material.

Acknowledgments

We thank Dr. Kathleen E. McGrath for scientific guidance in use of the ImageStreamX, Michael Silverstein and Margaret Young-man for help with image analysis, and Anne Koniski for technical support, particularly animal husbandry and collection of fetal blood samples. This work was supported by the National Institutes of Health and the National Institute of Diabetes and Digestive and Kidney Diseases (grant R01 DK09361 to J.P.), New York Stem Cell Science (to J.P.), and the Michael Napoleone Memorial Foundation.

References

1. Maximow A. Untersuchungen uber blut und bindegewebe 1. Die fruhesten entwicklungsstadien der blut- und binde-gewebszellan bein saugetierembryo, bis zum anfang der blutbilding unden leber. Arch Mikroskop Anat. 1909; 73:444–561.
2. Gulliver G. Observations on the sizes and shapes of the red corpuscles of the blood of vertebrates, with drawings of them to a uniform scale, and extended and revised tables of measurements. Proc Zool Soc London. 1875:474–495.

3. Palis J, Robertson S, Kennedy M, Wall C, Keller G. Development of erythroid and myeloid progenitors in the yolk sac and embryo proper of the mouse. Development. 1999; 126:5073–5084. [PubMed: 10529424]
4. Morioka K, Minamikawa-Tachino R. Temporal characteristics of the differentiation of embryonic erythroid cells in fetal peripheral blood of the Syrian hamster. Dev Growth Differ. 1993; 35:569–582.
5. Fraser ST, Isern J, Baron MH. Maturation and enucleation of primitive erythroblasts during mouse embryogenesis is accompanied by changes in cell-surface antigen expression. Blood. 2007; 109:343–352. [PubMed: 16940424]
6. Kingsley PD, Malik J, Fantauzzo KA, Palis J. Yolk sac-derived primitive erythroblasts enucleate during mammalian embryogenesis. Blood. 2004; 104:19–25. [PubMed: 15031208]
7. Mohandas N, Evans EA. Mechanical properties of the red cell membrane in relation to molecular structure and genetic defects. Annu Rev Biophys Biomol Struct. 1994; 23:787–818. [PubMed: 7919799]
8. Palek J, Sahr KE. Mutations of the red blood cell membrane proteins: From clinical evaluation to detection of the underlying genetic defect. Blood. 1992; 80:308–330. [PubMed: 1627793]
9. Leblond PF, LaCelle PL, Weed RI. Cellular deformability: a possible determinant of the normal release of maturing erythrocytes from the bone marrow. Blood. 1971; 37:40–46. [PubMed: 5539130]
10. Ganzoni A, Hillman RS, Finch CA. Maturation of the macroreticulocyte. Br J Haematol. 1969; 16:119–135. [PubMed: 5795203]
11. Shattil SJ, Cooper RA. Maturation of macroreticulocyte membranes in vivo. J Lab Clin Med. 1972; 79:215–227. [PubMed: 5009711]
12. Johnstone RM. Maturation of reticulocytes: formation of exosomes as a mechanism for shedding membrane proteins. Biochem Cell Biol. 1992; 70:179–190. [PubMed: 1515120]
13. Chasis JA, Prenant M, Leung A, Mohandas N. Membrane assembly and remodeling during reticulocyte maturation. Blood. 1989; 74:1112–1120. [PubMed: 2752157]
14. Waugh RE, Mantalaris A, Bauserman RG, Hwang WC, Wu JH. Membrane instability in late-stage erythropoiesis. Blood. 2001; 97:1869–1875. [PubMed: 11238131]
15. Fung YC, Tsang WCO, Patitucci P. High-resolution data on the geometry of red blood cells. Biorheol. 1981; 18:369–385.
16. Evans EA, Skalak R. Mechanics and thermodynamics of biomembranes. CRC Crit Rev Bioeng. 1979; 3:181–418. [PubMed: 393460]
17. Chien S, Sung KLP, Skalak R, Usami S. Theoretical and experimental studies on viscoelastic properties of erythrocyte membrane. Biophys J. 1978; 24:463–487. [PubMed: 728524]
18. Hwang WC, Waugh RE. Energy of dissociation of lipid bilayer from the membrane skeleton of red blood cells. Biophys J. 1997; 72:2669–2678. [PubMed: 9168042]
19. McGrath KE, Kingsley PD, Koniski AD, Porter RL, Bushnell TP, Palis J. Enucleation of primitive erythroid cells generates a transient population of “pyrenocytes” in the mammalian fetus. Blood. 2008; 111:2409–2417. [PubMed: 18032705]
20. Liu J, Guo X, Mohandas N, Chasis JA, An X. Membrane remodeling during reticulocyte maturation. Blood. 2010; 115:2021–2027. [PubMed: 20038785]
21. Isern J, Fraser ST, He Z, Zhang H, Baron MH. Dose-dependent regulation of primitive erythroid maturation and identity by the transcription factor Eklf. Blood. 2010; 116:3972–3980. [PubMed: 20720183]
22. Murdock RC, Reynolds C, Sarelius IH, Waugh RE. Adaptation and survival of surface-deprived red blood cells in mice. Am J Physiol Cell Physiol. 2000; 279:C970–C980. [PubMed: 11003577]
23. Butler J, Mohandas N, Waugh RE. Integral protein linkage and the bilayer-skeletal separation energy in red blood cells. Biophys J. 2008; 95:1826–1836. [PubMed: 18390600]
24. Agre P, Casella JF, Zinkham WH, McMillan C, Bennett V. Inheritance pattern and clinical response to splenectomy as a reflection of erythro-cyte spectrin deficiency in hereditary spherocytosis. New Engl J Med. 1986; 315:1579–1583. [PubMed: 3785322]

25. Waugh RE, LaCelle PL. Abnormalities in the membrane material properties of hereditary spherocytes. J Biomech Eng. 1980; 102:240–246. [PubMed: 19530807]

26. Chasis JA, Mohandas N. Erythrocyte membrane deformability and stability: two distinct membrane properties that are independently regulated by skeletal protein associations. J Cell Biol. 1986; 103:343–350. [PubMed: 3733870]

27. Hochmuth RM, Marcus WD. Membrane tethers formed from blood cells with available area and determination of their adhesion energy. Biophys J. 2002; 82:2964–2969. [PubMed: 12023219]

28. Keerthivasan G, Small S, Liu H, Wickrema A, Crispino JD. Vesicle trafficking plays a novel role in erythroblast enucleation. Blood. 2010; 116:3331–3340. [PubMed: 20644112]

29. Blanc L, De Gassart A, Geminard C, Bette-Bobillo P, Vidal M. Exosome release by reticulocytes–an integral part of the red blood cell differentiation system. Blood Cells Mol Dis. 2005; 35:21–26. [PubMed: 15946868]

30. Mohandas N, Chasis JA. The erythroid niche: molecular processes occurring within erythroblastic islands. Transfus Clin Biol. 2010; 17:110–111. [PubMed: 20655267]

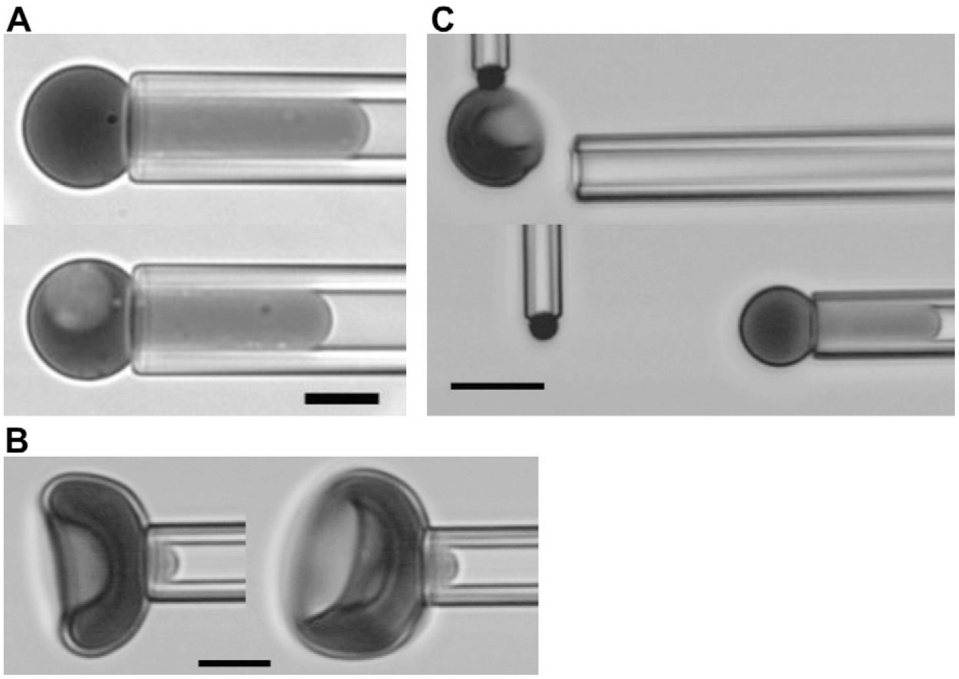

Figure 1.

Images of experimental procedures. (**A**) Measurement of area and volume. Cells are aspirated with sufficient pressure to form a spherical portion outside the pipette and a cylindrical projection within the pipette. The outer diameter of the spherical part and the length of the projection are used to calculate area and volume from the given equations. (**B**) Membrane shear modulus is determined by measuring the length of the cell projection in the pipette as a function of small increases in pressure. Cells with and without nuclei from an E15.5 sample are shown. (**C**) The stability of the bilayer skeletal interaction is measured by forming tethers from the cell surface. The cell is aspirated into the pipette and allowed to adhere to a target bead held at the tip of a microcantilever. The deflection of the cantilever from its rest position provides a measure of the tethering force. Changes in the aspiration pressure holding the cell in the pipette results in changes in the membrane tension. (**A, B**) Images obtained using a Nikon TE2000-E [436 nm monochromatic illumination, 100× 1.45 NA oil-immersion objective], Roper Quantem512SC digital camera, and Elements software (Nikon Instruments, Melville, NY); scale bar = 5 μm. (**C**) Images obtained with Olympus I×70 microscope [with 40 × 0.6 NA objective, 436 nm monochromatic illumination] and Hamamatsu C2400 CCD camera with background subtraction and brightness and contrast adjustments; scale bar =10 μm.)

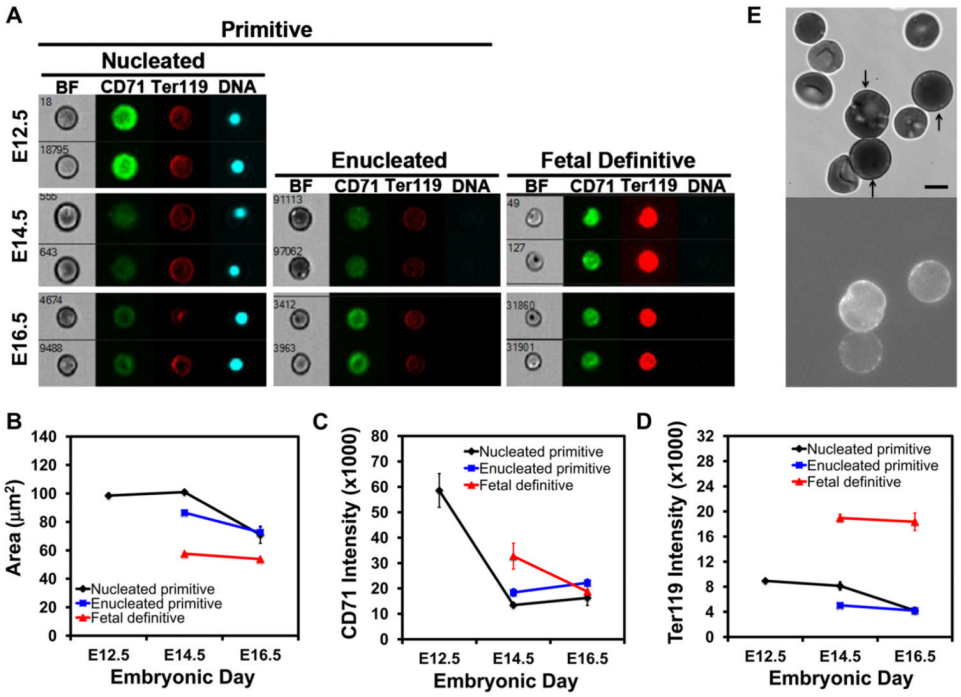

Figure 2.

Terminal maturation of primitive erythroid cells. (**A**) Representative images of circulating erythroid cells at E12.5, E14.5, and E16.5 of mouse gestation captured on the ImageStreamX imaging flow cytometer with a 0.75NA 40× objective lens. Cells were stained with Ter119-PECy7, CD71-FITC, and DRAQ5. (**B**) Changes in cell area of nucleated and enucleated primitive erythroid cells and enucleated definitive erythroid cells quantified by imaging flow cytometry. (**C**) Changes in surface expression of CD71 on primitive and definitive erythroid cells during their terminal maturation. The decrease inCD71 intensity on the surface of primitive erythroid cells between E12.5 and E14.5 is statistically significant (*t* test, $p = 0.02$), but the slight increase in the data between E14.5 and E16.5 is not significant (*t* test, $p = 0.28$). (**D**) Changes in Ter119 cell surface expression in primitive and definitive erythroid cells during their terminal maturation. Data in **B, C,** and **D** were derived from replicate measurements on three (E16.5) or four (E12.5 and E14.5) different embryos. Area represents the projected area of the cell in the image. Intensity is the median total intensity for the cells measured in arbitrary units. (**E**) Video-micrograph of CD9-labeled primary primitive erythroid cells. Bright-field images were obtained as for Figures 1A and 1B. Fluorescence images were obtained using the Nikon TE 2000-E microscope with a 100× 1.45 NA oil-immersion objective, and captured with a Roper Quantem 512SC digital camera using Elements software for a 900-ms exposure and multiplier of 700. Because definitive erythroid cells in the sample do not label, this methodology provided an objective method for identifying primitive erythroid cells. Scale bar = 5 μm.

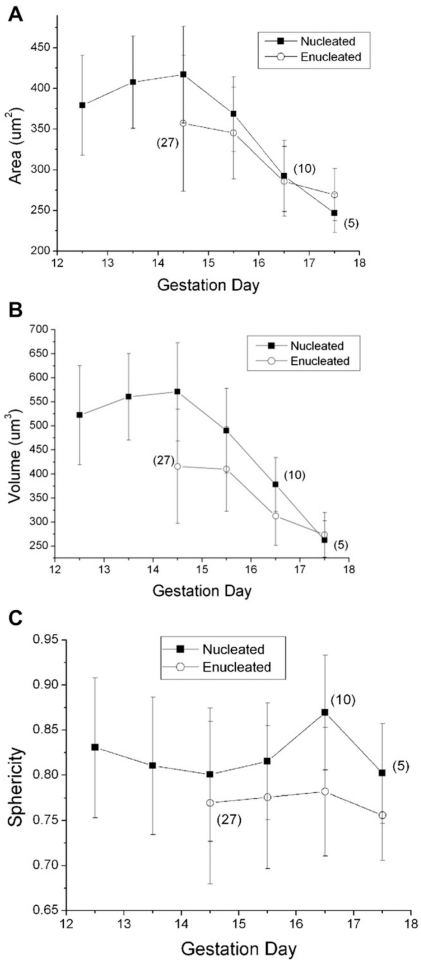

Figure 3.

Changes in cell dimensions with gestational age. There is little or no change in cell surface area or volume between E12.5 and E14.5, but thereafter there is an approximately linear decrease in both area and volume. Open symbols represent data for enucleated cells; filled symbols correspond to data for nucleated cells. In contrast to the large changes in area and volume, there was little change in the sphericity of cells with maturation, except for a decrease accompanying enucleation. Numbers in parentheses indicate the number of cells tested when sample size was less than 100. Error bars represent mean ± SD.

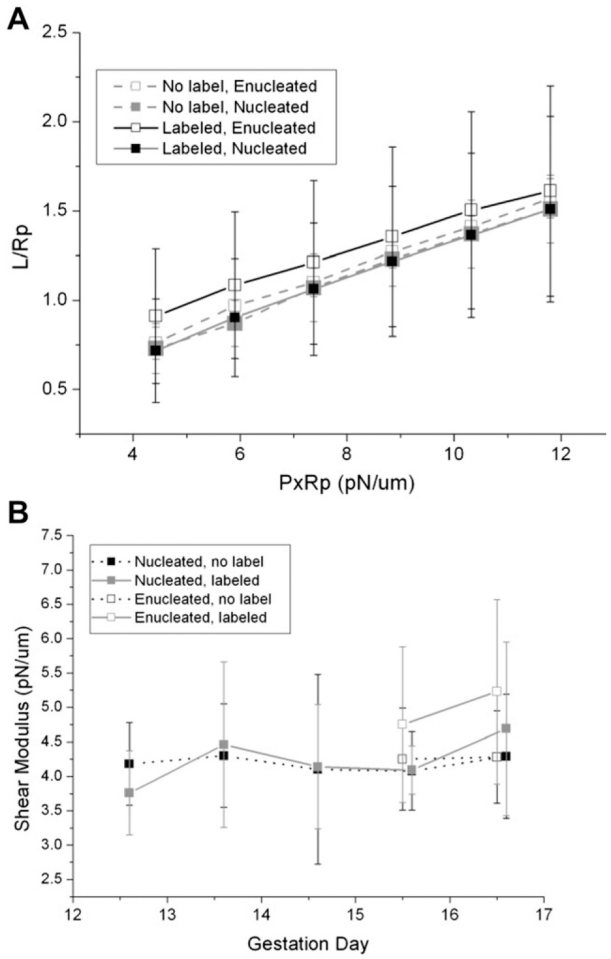

Figure 4.

Membrane deformability measurements. (**A**) Measurements of the projection length divided by pipette radius versus aspiration pressure multiplied by the pipette radius for circulating nucleated and enucleated primitive erythroid cells at E15.5 of gestation. Open symbols represent data from enucleated cells, and filled symbols represent data from nucleated cells. Cells selected on the basis of size without CD9 label (gray, dashed lines) showed the same behavior as cells labeled for CD9 (black, solid lines). (**B**) Shear modulus as a function of erythroid cell maturity. Each data point represents the mean of approximately 10 cells, and error bars indicate SD. ANOVA revealed no significant differences between cells labeled for CD9 or unlabeled, whether cells were nucleated or enucleated, or across different days of gestation.

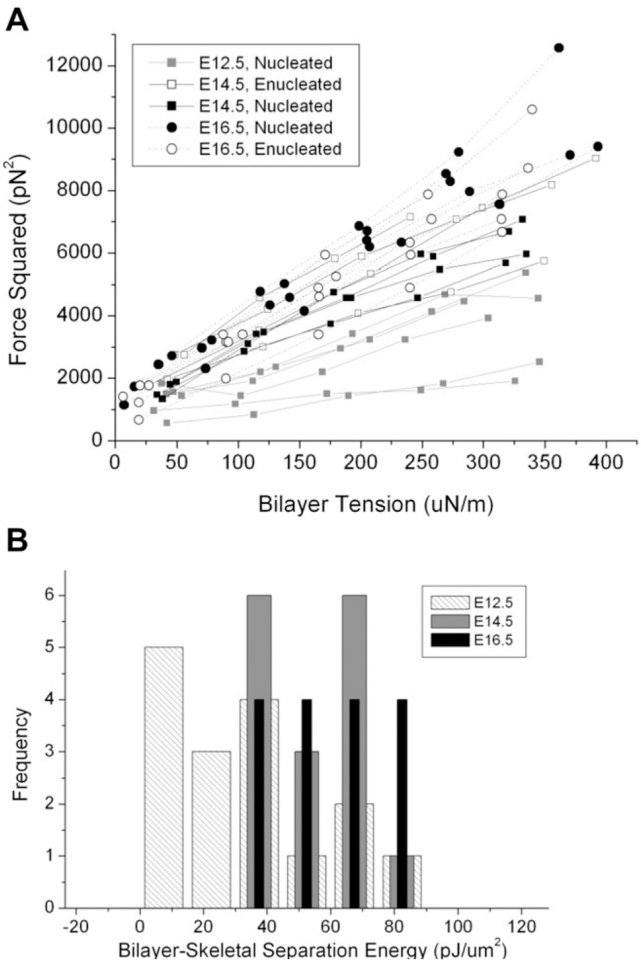

Figure 5.

Bilayer-skeletal separation measurements. (**A**) The square of the tethering force is plotted as a function of the tension in the membrane bilayer of primitive erythroid cells at E12.5, E14.5, and E16.5. The expected linear relationship was observed for nearly all cells. The change in slope from E12.5 through E16.5 most likely reflects loss of internal structures that interfere with an accurate determination of the membrane tension. The mean value of the y-axis intercept increases with maturity, suggesting a progressive increase in membrane stability with maturation. (**B**) Histogram of the measured values for the bilayer skeletal separation energy W_{sk}. Light hatched bars = E12.5; medium gray bars = E14.5; black bars = E16.5. The mean energy for E12.5 cells is significantly lower than the energy for E16.5 cells (ANOVA).

Table 1

Area, volume, and sphericity of primitive erythroid cells at different gestational stages

Age (embryonic day)	Area (mm^2)	SD (mm^2)	Volume (mm^3)	SD (mm^3)	Sphericity	SD	Count
Nucleated cells							
12.5	379.2	61.3	522.1	103.1	0.831	0.078	363
13.5	407.7	56.6	560.3	90.1	0.810	0.076	322
14.5	416.9	59.5	570.7	102.3	0.801	0.074	435
15.5	368.4	45.8	490.0	87.8	0.815	0.065	182
16.5	292.3	43.7	378.1	56.1	0.869	0.064	10
17.5	246.8	23.9	262.2	40.6	0.802	0.055	5
Enucleated cells							
12.5	—	—	—	—	—	—	0
13.5	—	—	—	—	—	—	0
14.5	357.0	83.4	415.9	118.6	0.770	0.090	27
15.5	345.1	56.4	410.4	87.7	0.776	0.079	147
16.5	285.8	42.8	312.8	61.0	0.782	0.071	325
17.5	269.4	32.0	273.3	46.8	0.756	0.050	198

Cells were aspirated into micropipettes until the portion of the cell outside the pipette became spherical. The cell area, volume and sphericity were calculated from measured cell dimensions according to Equations 1–3. The mean, standard deviation and number of cells measured are listed for the different days of gestation (age).

Table 2
Energy of bilayer skeletal separation at different gestational stages

Maturational stage	W_{sk} (pJ/μm^2)	SD (pJ/μm^2)	n
E12.5	30.4	12.0	17
E14.5	49.1	22.4	17
E16.5	53.0	21.9	16

E = embryonic day.

The bilayer skeletal separation energy was determined by linear regression to the tether force squared as a function of the bilayer tension for individual cells. (See Equations 5–8, Fig. 5A.) The mean, standard deviation and number of cells measured are given for three different days of gestation.